XVII European Conference
ECSMGE 2019
Reykjavik
on Soil Mechanics
and Geotechnical Engineering

Reanalysis of some in situ compaction test results
Réanalyse de certains résultats d'essais de compactage in situ

E. Imre
Óbuda University, Budapest Hungary

J. Lorincz, P. Q. Trang
BME, Budapest Hungary

F. Casini[1], G. Guida[2]
[1]*Università di Roma Tor Vergata* [2]*Università Niccolò Cusano, Italy*

Stephen Fityus
University of Newcastle, Australia

D. Barreto
Edinburgh Napier University, U.K

V. P. Singh
A. M. University, USA

ABSTRACT: Brandl (1977) presents the grading curve results of an investigation of particle disintegration of natural sandy gravel and crushed stone bedding courses due to *in situ* compaction and the action of construction traffic in different civil engineering applications. The work also includes a method to predict the disintegration behaviour of these materials, on the basis of simple laboratory investigations. The concerning compaction are presented in terms of grading curves. The entropy coordinates were computed for the grading curves, before and after compaction. According to the results, the base entropy S_o, which is a kind of dimensionless mean log diameter, is decreasing during compaction, the entropy increment is increasing according to the entropy principle. Since the grading curve difference and entropy path depend on the grain material and the compaction work, the latter can be characterized if the formers are known.

RÉSUMÉ: Brandl (1977) présente les la distributions du grain d'une étude sur la désintégration des particules dans les couches de litière de gravier sableux et de pierre concassée naturelles due au compactage in situ et à l'action du trafic de construction dans différentes applications de génie civil. Le travail comprend également une méthode permettant de prédire le comportement à la désintégration de ces matériaux, sur la base de simples analyses de laboratoire. Les compactages concernés sont présentés en termes de courbes de nivellement. Les coordonnées d'entropie pour les sols testés sont calculée, avant et après compactage. Selon les résultats, l'entropie de base, qui est une sorte de diamètre de log moyen sans dimension, diminue lors du compactage, l'incrément d'entropie augmente selon le principe de l'entropie. La variation de la distribution du grain dépend du matériau de grain et du travail de compactage, le travail de compactage peut être caractérisé si les formeurs sont connus.

Keywords: earthwork, compaction, fractal dimension, grading entropy, natural soils

1 INTRODUCTION

The directional properties of natural or spontaneous processes is investigated in a series of papers related to particle breakage (Lorincz et al, 2005 and 2018) and natural wheatering (Imre and Fityus 2018) and particle disintegration due to fragmentation.

In this paper the concept of grading entropy is applied to a dozen of road-construction sites and the samples taken from these sites for grading curve measurement before and after compaction.

The aim of the research was to test the effect of compaction on the grading curve. Similar behaviour was encountered due to compaction, as during fragmentation in nature or breakage in lab condition: decrease in the mean diameter and an increase in the entropy increment value.

2 GRADING ENTROPY

2.1 The space of the grading curves

The grading curve is the distribution of the log diameter of the grains by dry weight. In the grading curve measurement the sieve hole diameters are doubled. In the abstract fraction system the diameter range for fraction j (j =1, 2...j see Table 1, Lorincz (1986)) are defined by using the integer powers of the number 2:

$$2^j d_0 \geq d > 2^{j-1} d_0, \qquad (1)$$

where d_0 is the smallest diameter which may be equal to the height of the SiO_4 tetrahedron. The relative frequencies of the fractions x_i ($i = 1, 2, ..N$) fulfil the following equation:

$$\sum_{i=1}^{N} x_i = 1, \qquad x_i \geq 0, \; N \geq 1 \qquad (2)$$

Table 1. Fractions

j	1		23	24
Limits in d_o	*1* to 2		2^{22} to ^{23}	2^{23} to 2^{24}
S_{oj} [-]	1		23	24

where the integer variable N – the number of the fractions between the finest and coarsest non-zero fractions – is used. The relative frequencies x_i can be identified with the barycentre coordinates of the points of an N-1 dimensional, closed simplex (which is the N-1 dimensional analogy of the triangle or tetrahedron, the 2 and 3 dimensional instances). The vertices represent the fractions, the 2 dimensional edges are related to the two-mixtures etc (Figs. 1-2(a)). The sub-simplexes of a simplex are partly continuous, and partly gap-graded. The continuous sub-simplexes have a lattice structure, as is indicated in Figure 2.

2.2 Entropy parameters

The grading entropy S is a statistical entropy, modified for the unequal cells, since the sieves are doubled (Lorincz, 1986). It is a sum:

$$S = S_0 + \Delta S \qquad (3)$$

where S_0 is called the base entropy and ΔS the entropy increment. The base entropy:

$$S_0 = \sum x_i S_{0i} = \sum x_i i \qquad (4)$$

where S_{0k} is entropy of the *j*-th is equal to *j*. The normalized or relative base entropy *A*:

$$A = \frac{S_o - S_{o\min}}{S_{o\max} - S_{o\min}} \qquad (5)$$

where S_{0max} and S_{0min} are the entropies of the largest and the smallest fractions, respectively. The entropy increment ΔS is:

$$\Delta S = -\frac{1}{\ln 2} \sum_{x_i \neq 0} x_i \ln x_i. \qquad (6)$$

which varies between 0 and ln$N$/ln2, depending on the fraction number *N*. The normalized entropy increment *B:*

$$B = \frac{\Delta S}{\ln N} \qquad (7)$$

2.3 Entropy diagrams

Any grading curve can be represented as a single point in terms of the entropy coordinates. Any grading curve can be represented as a single point in terms of the entropy coordinates (Figs. 2(b)-3). Four maps can be defined between the N-1 dimensional, open simplex (fixed N) and the two dimensional real Euclidean space, the non-normalized $\Delta \rightarrow$ [$S_0, \Delta S$], normalized $\Delta \rightarrow [A, B]$, partly nor malized $\Delta \rightarrow [A, \Delta S]$ or [S_0, B].

The diagram is compact, like the simplex. The inverse image of the regular values is similar to an N-3 dimensional sphere, "centered" to the optimal point (Figs 2, 3). The inverse image of the the maximum normalized entropy increment lines B is the optimal line (Fig 2).

The optimal grading curve (Figs. 1, 4) or simplex point with maximal B for a specified A is unique since the entropy increment B is strictly concave function. The optimal   point maps at fixed A on the maximum B:

$$x_1 = \frac{1}{\sum_{j=1}^{N} a^{j-1}} = \frac{1-a}{1-a^N}, \quad x_j = x_1 \, a^{j-1} \tag{8}$$

where parameter a is the root of the following equation :

$$y = \sum_{j=1}^{N} a^{j-1}[j-1-A(N-1)] = 0. \tag{9}$$

The single positive root a varies continuously between 0 and ∞ as A varies between 0 and 1, $a=1$ at the symmetry point ($A=0.5$) and $a>1$ on the $A>0.5$ side of the diagram.

2.4 Stability criterion

On the basis of the suffosion test results, the three basic types of soil structures were related to three domains of the partly normalized entropy diagram (Fig 4). The physical content of criterion is that parameter A expresses the proportion of the large grains, which form

structure if they are present in large enough quantity. If $A < 2/3$, no structure of the large grains is present, the coarse particles "float" in the matrix of the fines. In the transitional zone, the coarse particles start to form a stable skeleton. In the stable zone, the structure of larger particles is inherently stable. The division connects the maximum entropy points with fraction number less than N (Figure 4, Table 2).

Table 2. The A coordinate of the maximum S point

N [-]	2	3	4	5
A [-]	0,667	0,714	0,756	0,790
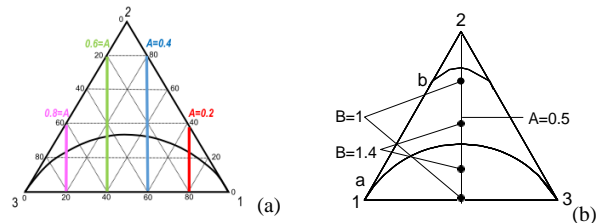
Figure 1. The 3- fraction soils N=3 in the triangle diagram with the optimal line 'a'. (a) to (b). Points with fixed A and, points with fixed A and B..
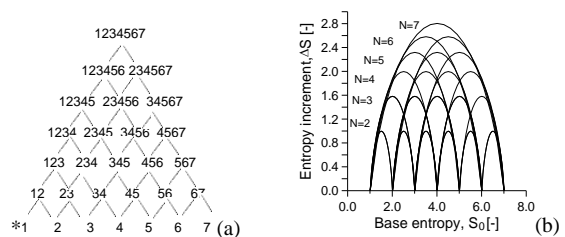
Figure 2. (a) Soils with N=7. Lattice of ,continuous' sub-simplexes (integers: fractions).(b) Soils with N=7, the image of the optimal lines of continuous sub-simplexes in the non-normalised entropy diagram.
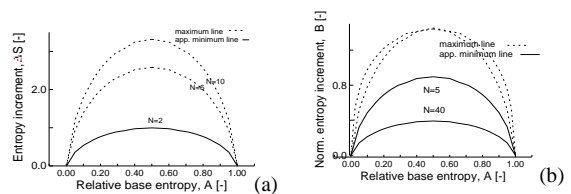
Figure 3. (a) to (b) Partly-normalized and. normalized diagrams, maximum lines: dashed line, appr. minimum lines: solid lines.
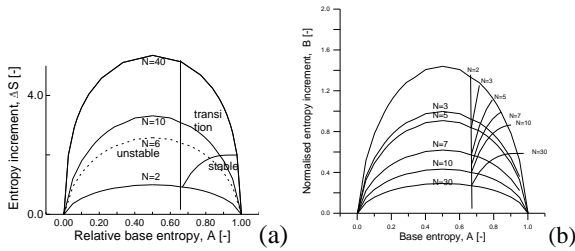
Figure 4. Internal stability criterion in the (a) partly normalized and (b) normalized diagram. (In the normalised diagram, the maximum line is approximately the same for all N, the image of edge 1-N depends on N, the curved limit lines between the unstable and transition zones depends on N.)

2.5 Discontinuity of the path

If N varies, the non-normalized entropy path of the grading curve in terms of $[S_0, \Delta S]$ is continuous. However, the normalized entropy path of the grading curve in terms of $[A,B]$ is not continuous. Some formulae can be derived for the discontinuity. If some i zero fractions are added from the smaller side, a discontinuity in the entropy diagram point is encountered:

$$B(N) - B(N+i) = \Delta S(N) \frac{1 - \dfrac{\ln N}{\ln N + i}}{\ln N} \qquad (10)$$

$$(11)$$

3 METHODS AND RESULTS

3.1 Methods

Brandl (1977) presents the grading curve results of an investigation of particle disintegration of natural sandy gravel and crushed stone bedding courses due to *in situ* compaction and the action of construction traffic in a dozen of sites.

The grading curves were digitalized and, the entropy coordinates (base entropy S_0 and entropy increment ΔS, relative base entropy A and normalised entropy increment B) were calculated in 3 ways.

First $N = 11$ to 12 fractions were assumed, the smalls appearing after compaction were neglected.

The theoretical smallest diameter (minimum grain size) is limited at a few microns at crushing (Kendall, 1978). Using this fact, the fines after compaction were taken into account either approximately, by assuming zero fractions up to the theoretical a smallest diameter limit (minimum grain size) or the 'precise' distribution for 18 non-zero fraction sizes was determined by fitting a Weibull distribution (Figure 8, see eg.,Guida at al, 2016).

3.2 Results

Some of the original grading curves are presented in Figure 5 as envelopes of the grading curves for the tested soils. Curves 1 and 2 are related to the states after and before compaction, resp. Results show that due to compaction, the largest fraction may vanish, which is not experienced in laboratory breakage tests due to the cushion effect.

*Table 3. Entropy parameter computations, upper envelopes, N=10 to 12, *:N=18.*

Fig/ page	S_o [-]		ΔS [-]		A [-]	
	2	1	2	1	2	1*
42/40	8,1	6,6	3,1	3,1	0,7	0,84
43/41	8,1	7,0	3,2	3,3	0,6	0,79
61/53	8,2	6,5	3,2	3,2	0,7	0,84
125/107	9,0	8,1	3,0	3,1	0,7	0,84
126/108	7,8	7,1	3,1	3,3	0,7	0,84
128/109	8,7	7,0	2,9	3,1	0,8	0,89
152/125	5,7	5,4	2,8	2,8	0,6	0,79
152/125	7,5	6,6	2,9	2,9	0,7	0,84
135/113	7,7	7,1	3,0	3,2	0,7	0,84
144/120	7,7	7,1	3,1	3,1	0,7	0,84
157/130	8,9	7,4	3,0	3,1	0,7	0,84
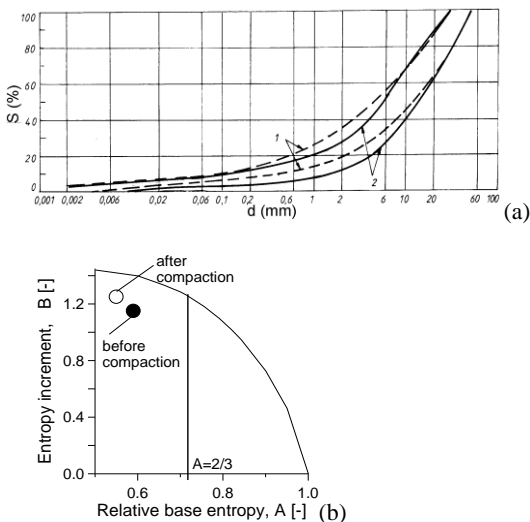
Figure 5. (a) The grading curves shown in Figure 23 on page 30 in Brandl (1977), lower and upper envelopes, 1:after, 2:before. (b) The normalized diagram, lower envelope, fines neglected.
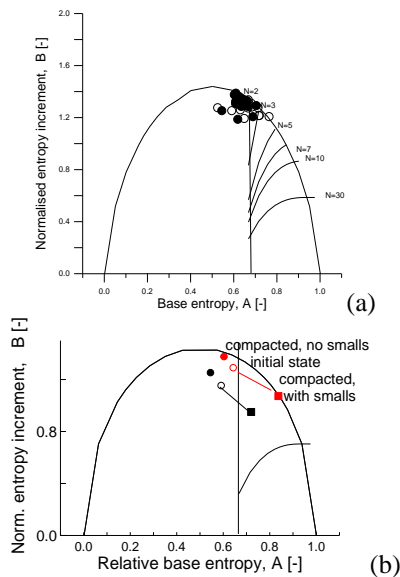
Figure 7. Data in the normalised diagram. Open symbol: before, full symbol:after compaction (a) The smalls are neglected after compaction, N=10 to 12,. (b) Zero smaller fractions after compaction (N=18).
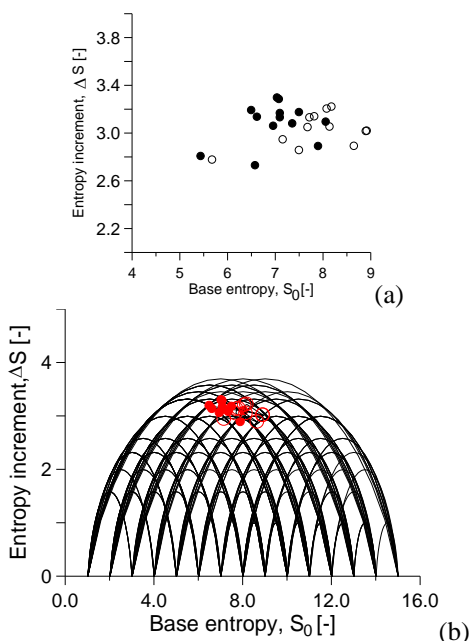
Figure 6. Non-normalised coordinates. Open symbol: before, full symbol: after compaction. (a) (b) Non-normalised diagram, diagram N=10 to 12.
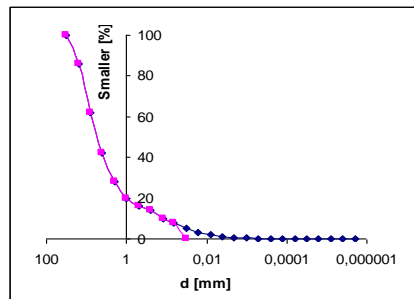
Figure 8. The result of model fitting assuming 18 fractions (resulting in about 0.06 difference in ∆S).

The non-normalized entropy coordinates were calculated before and after compaction, the results are shown in Table 3 and Figures 6 to 8. The base entropy S_o decreased, the entropy increment ΔS increased during breakage. The mean decrease in S_0 was about ~ 1,0, the mean increase in ΔS was~0,08. By interpolating the fine fractions (Figure 8), the fitted curve coordinates showed this tendency in a more pronounced way, results were influenced by the neglected smallest grains.

Table 4. The time evolution of the difference between the top and sub layers

S_{0base} - S_{0top} [-]	ΔS_{top} - ΔS_{base} [-]	t [year]
1,46		undisturbed
2,01	0,04	0 (control)
2,11	0,18	8
2,35	0,16	14
	0,73	undisturbed

The normalized entropy coordinates were calculated before and after compaction, the results are shown in Table 3 and Figure 7.

When the fines were approximately or precisely taken into account after compaction, the relative base entropy A and the normalised entropy increment B were significantly different, as follows.

The soil became internally transitionally stable after compaction if the apperence of smaller fractions were assumed as zero fractions up to the foregoing crushing limit.

4 DISCUSSION

4.1 The effect of wheatering

The use of soil grading entropy as a measure of soil texture maturity was investigated (Figure 9, Table 4, Imre and Fityus, 2018). A series of mine-spoil samples were collected from topsoils and subsoils at sites of mine rehabilitation that had been established for different periods of time.

Time evolution of the topsoil-subsoil difference showed a definite time variation, both in ΔS and S_0. The difference in ΔS was very small after remoulding (0.04) then it was monotonic increasing with time up to 0.16. Its tentative maximum is in the undisturbed or most mature value (0,73). The difference in ΔS between the top and the sub layer seems to be a good maturity variable. The subsoil-topsoil difference in S_0 increased with time, also.

(a)

(b)
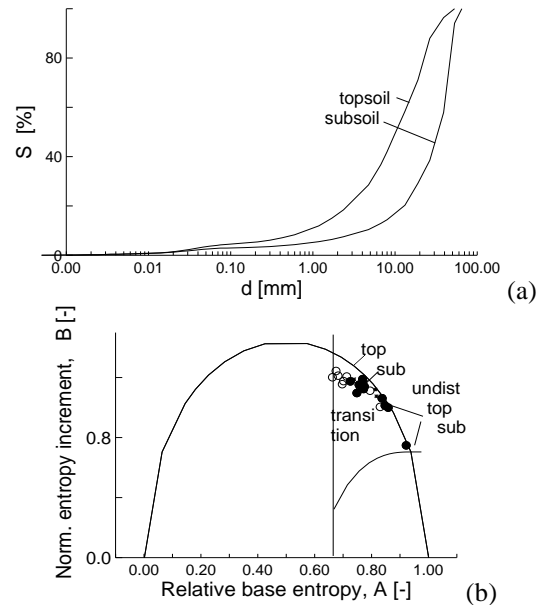
Figure 9. Degradation of natural waste rock in open pit mine rehabilitation. (a) The grading curves (b). Topsoil (open) and subsoil (closed) sample pairs in the N=17 in normalized diagram.

4.2 Laboratory breakage tests

In laboratory multicompression breakage tests made on different materials (Figure 10a to c, Figure 11, Lorincz et al, 2005 and 2018, Guida et al, 2016), moreover, in shear tests (see eg., Coop et al, 2004), the following very similar experiences are encountered.

During the test, the number of the fractions is increasing, the largest fraction is not vanishing due to the 'cushioning effect'. The base entropy S_o decreases, the entropy increment ΔS strictly monotonically increases during breakage. The normalized entropy path is different, if the number of the fractions is changing. The jump is related to $1- A$, the path is drifted into the more stable part of the diagram (Figure 10c).

Starting from the same initial grading but using different materials, the normalized entropy path seems to be independent of the type of rock material in breakage tests. The type of the rock can be characterized by the rate of breakage which can be measured precisely by the entropy coordinates (Lorincz et al, 2018).

(a)

(b)

(c)
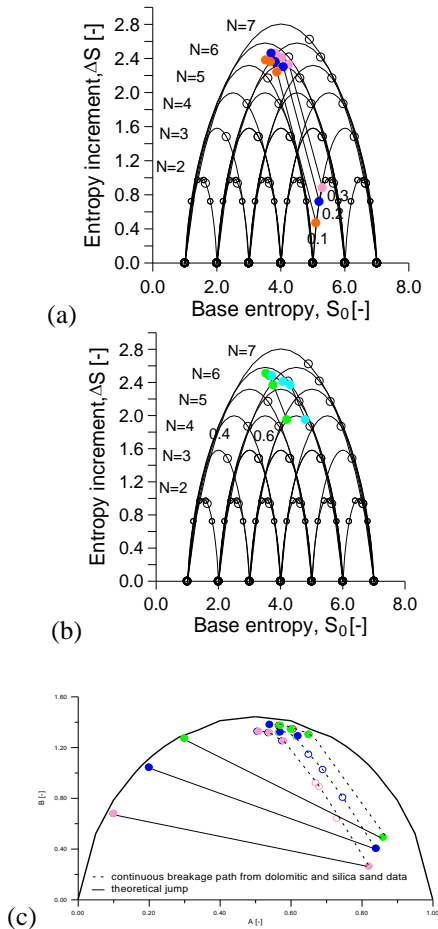
Figure 10. Entropy path, 30 crushing treatments. (a) to (b) Non-normalized paths for carbonate and silica soils. (c) The normalised paths. open circles: silica sand, full circles: carbonate sand. The computed jump in solid line. (Lorincz et al, 2018).
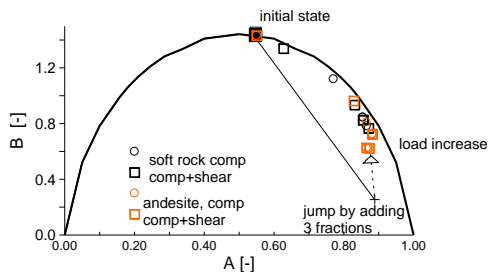
Figure 11. The normalised entropy paths for soft and hard rocks in compression and shear tests.) The computed jump in solid line (Lorincz et al, 2018).

4.3 Linking optimal and fractal

It is shown by Imre and Talata (2017) that the optimal grading curves have finite fractal distribution. The fractal dimension n varies between 3 and $-\infty$ on the $A>0.5$ side and between 3 and $-\infty$ on the $A<0.5$ side of the diagram.

The n depends on N except at the symmetry point of the diagram ($A = 0.5$, $B = 1/\ln2$, $n = 3$). The global maximum of S is related to such an optimal point where $n = 2$ (Table 2).

The soil is unstable in terms of grading entropy criterion if A is less than A=0.66. The related n depends on N, it is 2,62 for N=7, it is 2,25 for N=3, it is 2.96 for N=30.

The fractal distribution is stable if $n< 2$ (indepently of N, A). The transitional stability zone is situated between the fractal dimension at A=0.66 varying in the function of N, and fractal dimension n =2. Due to the entropy principle, soils in nature are generally near-fractal.

5 CONCLUSION

The results of the analysis related to the effect of compaction on the grading curve (Brandl, 1977) in terms of grading entropy can be summarized in detail as follows.

1. The normalized entropy coordinates before and after compactions at 11 sites were computed such that the distribution of smalls (being below ~8 %) was neglected. The earth work materials - natural sandy gravel and crushed stone mixtures at a dozen of sites – were surprisingly with near-fractal grain size distribution.

2. The soil was internally stable after compaction if the apperence of smaller fractions was assumed as zero fractions up to the crushing limit or the zero fractions were interpolated.

3. The entropy path was similar in compaction, wheatering and laboratory breakage tests. The base entropy S_o decreased, the entropy increment ΔS increased, comparably.

Reanalysing a previous wheatering study it is found (Table 4) that the topsoil-base-soil difference ΔS characterized the wheatering of the earthwork. The ΔS was very small after construction (0.04), increased up to 0.16 within a few years. The the decrease in S_0 was about 0.35. In compaction, the mean decrease in S_0 was about ~ 1,0, the mean increase in ΔS was~0,08. In breakage, the change in both parameters was slightly larger as shown in Figure 12.

It can be concluded that from the grading curves measured before and after compaction, the compaction work can be characterized if the some a priori grain material information is available. The characteristic grading entropy change related to the grain material under fixed energy input and test condition can be measured eg., in multistage breakage tests.

Some further research is suggested on the laboratory measurement of the various grain material characteristic relations in terms of grading entropy changes in breakage tests and, on the interpolation of grading curves for the fines up to the crushing limit.

6. REFERENCES

Brandl, H. 1977. Ungebundene Tragschichten im Strassenbau Heft 67 *Bundesministerium, Strassenforschung*. 188p.

Coop, M. R., Sorensen, K. K., Bodas Freitas, K. K. & G. 2004. Particle breakage during shearing of a carbonate sand. *Geotechnique* 54(3): 157-163.

Einav 2007. Breakage mechanics. J of the Mech. and Physics of Solids, 55: 1274-1297.

Guida G., Bartoli M., Casini F., Viggiani G.M.B. 2016. Weibull Distribution to Describe Grading Evolution of Materials with Crushable Grains. *Proc. Eng,* 158, pp. 75-80.

Hartmann W K, 1969. Terrestrial, lunar, and interplanetary rock fragmentation. *Icarus* 10, No. 2, 201–213.

Imre E, Talata I 2017. Some comments on fractal distributions and the grading entropy theory. *MAFIOK*. Budapest, Hungary, 2017.08.24-2017.08.26. Paper 13. 76 p.

Imre E. Barreto D. Talata I. Goudarzy, M. Rahemi, N. Baille W. Singh V. P. 2018. Fractal and optimal gradings and their relationship to internal stability. *IS Atlanta.*

Imre E, Fityus S 2018. The use of soil grading entropy as a measure of soil texture maturity. *Proc. XVI. DECGE* Skopje. 639-644.

Lorincz J, Imre E, Gálos M, Trang Q.P, Telekes G, Rajkai K, Fityus I. (2005) Grading entropy variation due to soil crushing. *Int. J of Geomech*. Vol 5. Number 4. p. 311-320.

Lorincz, J.; Imre, E.; Fityus, S.; Trang, P.Q.; Tarnai, T.; Talata, I.; Singh, V.P. The Grading Entropy-based Criteria for Structural Stability of Granular Materials and Filters. *Entropy* 2015, 17, 2781-2811.

Lorincz J, Imre E ; Trang P Q,. Gálos M, Kárpáti L, Talata I, Barreto d, Casini F, Guida G, 2018. A method for rock qualification. *Eng. Geol. Conf.* Budapest 2018 263-274.

Kendall, K. 1978. The impossibility of comminuting small particles by compression. *Nature* Vol 272. p. 710-711.
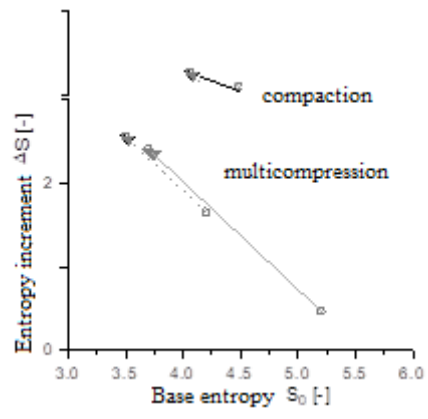
Figure 12. Comparing the entropy paths of the multicompression lab test (Figure 10, softer rock has longer path in the same testing condition) with mean compaction path vector derived from Table 3.